Commun. Theor. Phys. **72** (2020) 045501 (6pp) https://doi.org/10.1088/1572-9494/ab76fc

Boundary graphene layer effect on surface plasmon oscillations in a quantum plasma half-space

Raheleh Aboltaman[1,2,3] **and Mehran Shahmansouri**[1,2]

[1] Department of Physics, Faculty of Science, Arak University, Arak, PO Box 38156-8-8349, Iran
[2] Institute of Advanced Technology, Arak University, Arak, PO Box 38156-8-8349, Iran

E-mail: rahele.ab@gmail.com and mshmansouri@gmail.com

Received 26 August 2019, revised 14 January 2020
Accepted for publication 3 February 2020
Published 16 March 2020

Abstract

The effect of graphene on unique features of surface plasmon-polariton excitations near the interface of vacuum and quantum plasma half-space is explored using a quantum hydrodynamic model including the Fermi electron temperature and the quantum Bohm potential together with the full set of Maxwell equations. It is found that graphene as a conductive layer significantly modifies the propagation properties of surface waves by making a change on the corresponding wave dispersion relation. It is shown that the presence of graphene layer on the interface of vacuum and plasma leads to a blue-shift in the surface Plasmon frequency. The results of present study must be contributed to the modern electronic investigations.

Keywords: plasmon-polariton, quantum plasma, quantum hydrodynamic model, graphene, nano-electronic

(Some figures may appear in colour only in the online journal)

1. Introduction

The physical characteristics of surface waves has attracted a great interest in theoretical, numerical, and experimental investigations in many fields of plasma science and technology such as plasma spectroscopy, surface science, nano-electronic devices with surface Plasmons which can be excited and transmitted in metal thin films, laser physics, overdense plasma heating and so on [1–10]. These waves can propagate along the boundary of two different mediums with different signs of the real part of dielectric response function [11] and evanescent on either side of it. The existence of the linear electrostatic surface oscillations was first proved for a cold plasma half-space by Ritchie in 1957 [12] and for a cold cylindrical plasma columns by Trivelpiece and Gould in 1959 [13]. The effects of finite plasma temperature have also been considered [14–17] and the propagation of the surface waves on an unmagnetized quantum plasma half-space has been investigated by employing the quantum hydrodynamic (QHD) model which obtained from self-consistent Hartree equations [18] or from the phase-space Wigner–Poisson equations [19] conjugating with Maxwell–Poisson equations by Lazar *et al* [16] and Shahmansouri [17].

The electrostatic surface oscillations of free electrons near a plasma-dielectric surface is called surface Plasmon (SP) and it's linear coupling with photons is considered as a hybrid surface mode called surface Plasmon Polariton (SPP). SPs can provide a way of confining electromagnetic field to nanoscale structures and SPPs can be excited at frequencies ranging from 0 up to $\omega_{pe}/\sqrt{2}$ (in which ω_{pe} considered as the plasma frequency).

The quantum Fermi temperature and quantum electron tunneling (Bohm potential) effects should be considered, due to the great degree of miniaturization of nowadays electronic devices and also high number density in metallic plasmas or in solid-density plasma. On the other hand, the quantum effects can no longer be neglected since the thermal deBroglie wavelength of electrons is comparable to the average inter-particle distance of them. The dispersion relation of surface waves is profoundly affected by both the quantum Fermi

[3] Author to whom any correspondence should be addressed.

temperature and quantum electron tunneling effects [16, 17]. This is the case that makes the behavior of surface waves on quantum plasma half-space as an important issue in recent years. The fundamental properties of the surface waves in quantum plasma have been studied in the previous investigations [10, 16–33] under the influence of e.g. the quantum tunneling [10, 20–31], external magnetic field [20–22], collisional effects [24, 25], relativistic effects [26], spins [27–30], nonlocality effects [31] and exchange effects [17, 32 and 33].

A surprising property of graphene [34–43], a two dimensional (2D) monolayer of carbon atoms tightly packed in a hexagonal lattice, has attracted a great deal of attention for a wide range of electronic and electromagnetic applications. Interaction of the electrons with this wonderful atomic structure forces the charge carriers in graphene to act as an effective zeromass particle which can show photon-like dispersion in the low energy excitations [44]. The unique electron structure in which conduction and valance bands meet each other at the Dirac point is the origin of the extraordinary optical properties of graphene. The property of graphene can be tuned by chemical doping or electrical gating due to change in the value of the chemical potential μ_c or Fermi level E_f of graphene. The complex dynamic optical response of graphene consisting of interband and intraband contributions can be derived from Kubo formula [45–48]. By changing in the level of chemical potential, the imaginary part of conductivity can achieve negative and positive values [48], in different ranges of frequencies.

Here, only the intraband conductivity which dominates the low frequency process of graphene transition is included. Therefore, the optical conductivity of graphene ($\sigma_g \approx \sigma_{intra}$) is defined as follow [49–53]:

$$\sigma_{g,intra} = i\frac{e^2 k_B T}{\pi\hbar^2(\omega + 2i\tau^{-1})}\left[\frac{\mu_c}{k_B T} + 2\ln(e^{-\frac{\mu_c}{k_B T}} + 1)\right]. \quad (1)$$

In which ω is frequency of the incident light, T is temperature, k_B is Boltzmann constant, τ is relaxation time and, μ_c is chemical potential. For the gated or highly doped graphene ($|\mu_c| \gg k_B T$), the interband terms of the graphene conductivity have form [46]:

$$\sigma_{g,inter} = \frac{e^2}{4\hbar}\theta(\hbar\omega - 2|\mu_c|) + \frac{i}{\pi}\ln\left[\frac{2|\mu_c| - (\omega + 2i\tau^{-1})\hbar}{2|\mu_c| + (\omega + 2i\tau^{-1})\hbar}\right]. \quad (2)$$

Recent investigations reveal that low-cost metal-graphene composites [54–57] are promising materials in high-power electronics applications and can be widely used in digital and nanoelectronic devices. The bonding of graphene to metal substrates can be classified into two groups [54, 56]: (i) physisorption, in which the interaction between graphene and metals, such as Ag, Au, Cu, Al and Pt(111) is weak and preserves the graphene's linear dispersion band and Dirac cone. This weak adsorption on metal surfaces causes the Fermi level to shift from the conical points in graphene, leading to doping with either electrons or holes [56]. The difference of the graphene and metal work functions is the origin of this doping. The downward (upward) shift of Fermi-level means that holes (electrons) are transfer from the metal substrate to graphene (in order to equilibrate the Fermi levels), which causes p-type (n-type) doping. Graphene is p-type on Au and Pt and n-type on Ag, Al and Cu. (ii) chemisorptions, the metals Co, Ni and Pd bind graphene so strong that the electronic characteristics of graphene (the characteristic conical point at K) are disturbed. In this work we study the Au-graphene structure in which the basic characteristics of graphane remain unchanged. The rapid progress in this field necessitates a fundamental study of their interfacial structural and electronic coupling, which could be the key issue to determine their performance for engineering applications [54], for more information see [54–58].

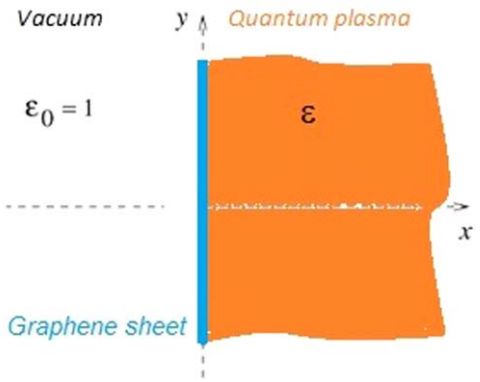

Figure 1. Schematic diagram of a quantum plasma half-space: the graphene sheet is located on the interface of plasma-vacuum at the plane $x = 0$, and the surface wave is propagating along the interface on y axis.

In this work, we investigate the effect of a graphene sheet which exactly placed on the boundary of quantum plasma half-space and vacuum (see figure 1), on the dispersion relation of the plasma surface waves (SPPs).

The outline of this paper is as follows: after introduction, in section 2, we derive the general dispersion relation of SPP which is strongly affected by the existence of graphene on the boundary and then, the dispersion relation is analyzed numerically and discussed in section 3. Finally, the outcomes of this paper are summarized in section 4.

2. Theoretical model

In grphene, two kinds of electrons named σ and π electrons can support Plasmons. 2D Plasmons (also named low energy Plasmons with energy <3 eV) which is responsible for intraband transitions, can appear in doped graphene while two other kinds of Plasmons (named as π and $\pi + \sigma$) exist in pristine graphene and also in higher energies (>3 eV) [58]. An interested frequency range for our model, cannot excite these two types of Plasmons in graphene, therefore we just focus on the metal (quantum plasma half-space) Plasmons. To investigate the dispersion properties in a quasineutral collisionless quantum plasma half-space (shown in figure 1) consisting of motionless ions (as a neutralizing background)

and fluid electrons, we use a macroscopic approach based on the linearized fluid equations, which is valid just in the weak $r_s \leqslant 0.1$ and moderate $0.1 < r_s \leqslant 1$ coupling (in which $r_s = e^2/\hbar v_F$ is a quantum coupling parameter or fine structure constant) [43], including the quantum statistical pressure and the quantum electron tunneling (the second and the third term in equation (4), respectively),

$$\frac{\partial n}{\partial t} + n_0 \nabla \cdot \boldsymbol{v} = 0, \tag{3}$$

$$\frac{\partial \boldsymbol{v}}{\partial t} = -\frac{e}{m}\boldsymbol{E} - \frac{v_{Fe}^2}{n_0}\nabla n + \frac{\hbar^2}{4m^2 n_0}\nabla\nabla^2 n, \tag{4}$$

and the full set of the Maxwell–Poisson equations for the electromagnetic fields,

$$\nabla \times \boldsymbol{E} = -\frac{1}{c}\frac{\partial \boldsymbol{B}}{\partial t}, \tag{5}$$

$$\nabla \times \boldsymbol{B} = \frac{1}{c}\frac{\partial \boldsymbol{E}}{\partial t} - \frac{4\pi n_0 e}{c}\boldsymbol{v}, \tag{6}$$

$$\nabla \cdot \boldsymbol{B} = 0, \tag{7}$$

$$\nabla \cdot \boldsymbol{E} = -4\pi e n. \tag{8}$$

In which n ($\ll n_0$) is a small electron density perturbation in the equilibrium number density n_0, e is the magnitude of the electron charge, m is the electron mass and the perturbed quantities $\boldsymbol{v}$, $\boldsymbol{E}$ and $\boldsymbol{B}$ are respectively the electron fluid velocity, the electric and magnetic fields. The surface wave propagates on the interface (which covered by a graphene layer) along the y axis. We will study the surface transverse magnetic (TM) wave so the field components are given by $\boldsymbol{E} = (E_x, E_y, 0)$ and $\boldsymbol{B} = (0, 0, B_z)$. In the following, by assuming that all the physical quantities vary as $\psi(x)\exp(\mathrm{i}k_y y - \mathrm{i}\omega t)$ in which $\psi(x) \equiv [N(x); U_x(x); U_y(x); E_x(x); E_y(x); B_z(x)]$ and by employing the time-space Fourier transformation of equations (3), (4) and (8), and by neglecting of the very slow non-local variations, i.e. $(k_y^{-2}(\partial^4/\partial x^4) \ll \partial^2/\partial x^2 \ll k_y^2)$ the following wave equation for the electron density can be obtained as:

$$\left[\frac{\mathrm{d}^2}{\mathrm{d}x^2} - \gamma_p^2\right]N(x) = 0, \tag{9}$$

where $\gamma_p = \sqrt{k_y^2 + (\omega_{pe}^2 - \omega^2)}/\sqrt{(v_{Fe}^2 + \hbar^2 k_y^2/4m^2)}$ defined as wave number in wave equation for the electron density and $\omega_{pe} = \sqrt{(4\pi n_0 e^2/m)}$ known as electron plasma frequency.

Then, the second-order differential equation for the magnetic field can be obtained by employing the Maxwell equations (5) and (6) and the momentum equation (4), as follow:

$$\left[\frac{\mathrm{d}^2}{\mathrm{d}x^2} - q_p^2\right]B(x) = 0, \tag{10}$$

in which the wave number q_P is given by $\sqrt{k_y^2 + (\omega_{pe}^2 - \omega^2)/c^2}$.

Equations (9) and (10) have the solutions of the following form:

$$N_v(x) = 0 \quad x < 0, \tag{11}$$

$$N_p(x) = A\exp(-\gamma_p x) \quad x > 0, \tag{12}$$

$$\boldsymbol{B}_v(x) = B_1\exp(q_v x), \quad x < 0, \tag{13}$$

$$\boldsymbol{B}_p(x) = B_2\exp(-q_p x) \quad x > 0, \tag{14}$$

where $q_v = \sqrt{k_y^2 - \left(\frac{\omega^2}{c^2}\right)}$. By using the Maxwell equation (4), the electric field of surface modes can also be obtained as follows:

$$\boldsymbol{E}_v(x) = \boldsymbol{D}_1\exp(q_v x) \quad x < 0, \tag{15}$$

$$\boldsymbol{E}_p(x) = \boldsymbol{D}_2\exp(-q_p x) \quad x > 0. \tag{16}$$

$$-4\pi eA\left(v_{Fe}^2 - \frac{\hbar^2(\gamma_p^2 - k_y^2)}{4m^2}\right) \times \frac{\exp(-\gamma_p x)}{\omega_{pe}^2 - \omega^2}(-\gamma_p\hat{i} + \mathrm{i}k_y\hat{j}).$$

In the aforementioned equations, $\boldsymbol{D}_1$ and $\boldsymbol{D}_2$ are constants given by $\boldsymbol{D}_1 = B_1(-c\omega/k_y\omega^2)(k_y^2\hat{i} + \mathrm{i}q_v k_y\hat{j})$ and $\boldsymbol{D}_2 = B_2(c\omega/k_y(\omega_{pe}^2 - \omega^2))(k_y^2\hat{i} - \mathrm{i}q_p k_y\hat{j})$, respectively.

In what follows, we just keep that part of solutions which disappear by moving away from the boundary in both regions. The boundary conditions for the electromagnetic field components will be modified by the existence of graphene sheet with conductivity σ_g on the plasma-vacuum interface, in the following form:

$$\hat{x} \times (B_{pz}|_{x=0^+} - B_{vz}|_{x=0^-}) = \frac{\sigma_g}{c}E_{vy}|_{x=0^-}, \tag{17}$$

$$E_{vy}|_{x=0^-} = E_{py}|_{x=0^+}. \tag{18}$$

By using the above matching conditions together with the boundary condition $v_x = 0$ at $x = 0$ for the electron velocity, the dispersion relation of the surface modes on our quantum plasma half-space system can be derived as follow:

$$\frac{k_y^2\omega_{pe}^2}{\left(\frac{q_v}{\omega^2}\left[1 + \mathrm{i}q_v\frac{\sigma_g}{\omega}\right]^{-1} - \frac{q_p}{(\omega_{pe}^2 - \omega^2)}\right)} + \gamma_p\omega^2(\omega_{pe}^2 - \omega^2) = 0. \tag{19}$$

To our knowledge, this is the first time that a dispersion relation of SPP mode on a quantum plasma half-space with a graphene sheet on the interface has been derived. In the absence of graphene ($\sigma_g \to 0$) this dispersion relation leads to that obtained by Kaw and McBride [15] (in the absence of quantum corrections) and Lazar *et al* [16] results. In the following we assume overcritical density plasmas (which happen in solid state plasma such as metals and semiconductors) by letting $(k_y^2 v_{Fe}^2 + \hbar^2 k_y^4/4m^2 \ll |\omega_{pe}^2 - \omega^2|)$, and then equation (19) reduces to the following form:

$$\frac{\omega^2}{\omega_{pe}^2 - \omega^2} = -\frac{\omega^2}{k_y^2 c^2} + \frac{2\sqrt{k_y^2 - \left(\frac{\omega^2}{c^2}\right)}}{\sqrt{\omega_{pe}^2 - \omega^2}}\left(v_{Fe}^2 + \frac{\hbar^2 k_y^2}{4m^2}\right)^{\frac{1}{2}} + \frac{1}{\left[1 + \mathrm{i}\frac{\sigma_g}{\omega}\left(\sqrt{k_y^2 - \left(\frac{\omega^2}{c^2}\right)}\right)\right]}. \tag{20}$$

Since in the standard metallic densities [59], quantum effects do not affect the transverse electromagnetic component of the surface modes, we restrict our attention to the electrostatic part of the surface waves only. In the electrostatic limit, or when $c \to \infty$, the general dispersion relation (20) leads to the following form:

$$\omega^2 = \frac{\omega_{\rm pe}^2}{2}\left(\frac{1}{\left[1 + {\rm i}k_y\frac{\sigma_{\rm g}}{\omega}\right]} + \frac{4k_y}{\sqrt{2}\,\omega_{\rm pe}}(v_{\rm Fe}^2 + \hbar^2 k_y^2/4m^2)^{\frac{1}{2}}\right). \tag{21}$$

Without quantum effects and in the absence of graphene sheet, equation (20) yields to the equation derived by Ritchie [14] for the surface electrostatic waves on a thermal plasma half-space. Moreover, in the case of cold classical plasma equation (21) leading to the well-known frequency of surface Plasmons $\omega = \omega_{\rm pe}/\sqrt{2}$.

3. Numerical analysis

By introducing the dimensionless quantities: $W = \omega/\omega_{\rm pe}$, $\Im = (\omega_{\rm pe}\tau)$, $K = k_y v_{\rm Fe}/\omega_{\rm pe}$ and the Plasmonic coupling parameter as $H = \hbar\omega_{\rm pe}/2m_e v_{\rm Fe}^2$, equation (21) can be rewritten as follow:

$$W^2 = \frac{1}{2}\left(\frac{1}{\left[1 + {\rm i}K\frac{\bar{\sigma}_{\rm g}}{W}\right]} + \frac{4K}{\sqrt{2}}(1 + K^2H^2)^{\frac{1}{2}}\right). \tag{22}$$

In which the normalized conductivity $\bar{\sigma}_{\rm g}$ define as $\bar{\sigma}_{\rm g} = {\rm i}\beta\xi/(W + 2{\rm i}\Im^{-1})$ where $\xi = e^2 k_{\rm B}T/\hbar^2 v_{\rm F}\omega_{\rm pe}$ and $\beta = (\mu_{\rm c}/k_{\rm B}T) + 2\ln(\exp(-\mu_{\rm c}/k_{\rm B}T) + 1)$.

We depict equation (22) by using the typical values of the gold metallic plasma at room temperature as follows [16, 59]: $n_0 = 5.9 \times 10^{22}\,{\rm cm}^{-3}$, $\omega_{\rm pe} = 1.37 \times 10^{16}\,{\rm s}^{-1}$ and $v_{\rm Fe} = 1.4 \times 10^8\,{\rm cm\,s}^{-1}$. For physisorbed graphene on Au metal, the mutual interaction is so weak that its electronic structure is unchanged and just the Fermi level (or chemical potential $\mu_{\rm c}$) shift from conical point and achieve to 0.2 eV [54–56] and using $\tau = 0.5$ ps for relaxation time of charge carriers [49–51]. Since graphene in our model supposed to be ungated and doped in low densities by gold metal, the optical conductivity of graphene is defined by intraband term of conductivity ($\sigma_{\rm g} \approx \sigma_{\rm intra}$, equation (1)). The above assumptions yields $W\Im \gg 1$, which help us to approximate the graphene conductivity (1) in the following form

$$\bar{\sigma}_{\rm g} = \frac{{\rm i}\beta\xi}{W}. \tag{23}$$

The above expression shows that the normalized conductivity becomes a pure imaginary (pure real) quantity for $W\Im \gg 1$ ($W\Im \ll 1$). In this case the wave frequency reduced to the following form as

$$W^2 = \frac{1}{2}\left(\frac{1}{1 - \beta\xi K/W^2} + \frac{4K}{\sqrt{2}}(1 + K^2H^2)^{1/2}\right). \tag{24}$$

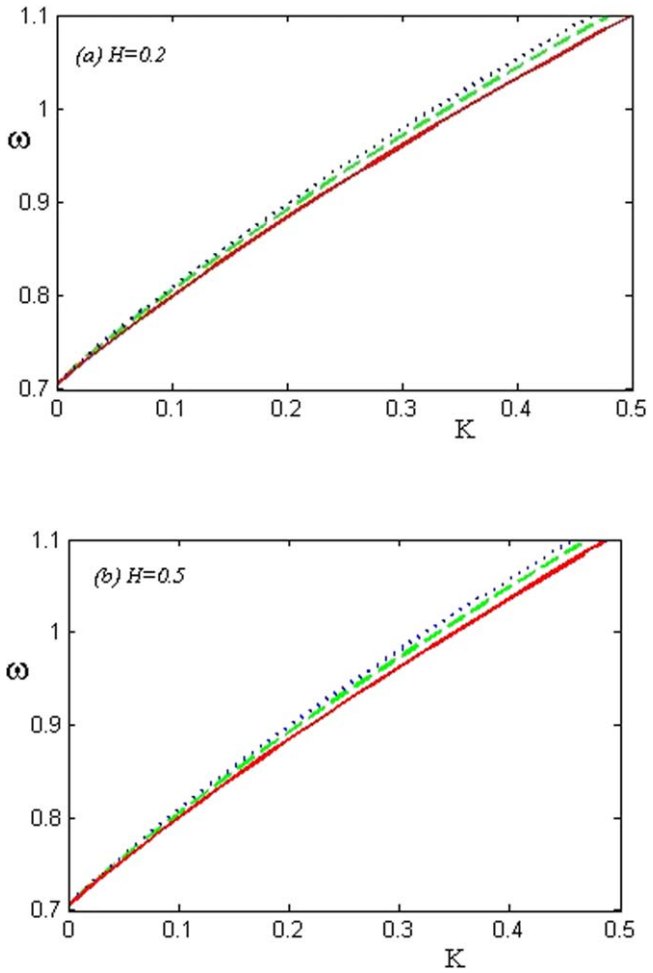

Figure 2. The normalized frequency of the surface plasmon waves W with respect to the normalized wave number K, for (a) $H = 0.2$ and (b) $H = 0.5$, and different values of parameter $\beta\xi$, as solid line refers to $\beta\xi = 0$, dashed line refers to $\beta\xi = 0.11$, and dotted line refer to $\beta\xi = 0.2$.

Then, in order to see how the frequency wave may be affected by the presence of the thin graphene layer, the normalized wave frequency W is depicted in figures 2 and 3, for different values of $\beta\xi$ and H, respectively.

Figure 2 represents the normalized wave frequency W of surface waves as a function of the normalized wavenumber K, in the presence of graphene layer for different values of the parameter $\beta\xi$. This figure represents that the frequency of surface Plasmon waves experiences an enhancement due to the presence of boundary graphene layer. For better comparison the Lazar *et al* [16] limit is included in this figure (solid line). The up-shift of the wave frequency increases with magnitude of the conductivity coefficient. The effect of the Plasmonic coupling parameter is included in panels (a) and (b) of figure 2. It is obvious that the wave frequency for higher values of H is takes greater values.

To see an obvious influence of the quantum effects on the wave frequency, figure 3 is depicted for different values of H, beside the limits of Lazar *et al* [16] (marker o) and Ritchie [14] (marker ×), for $\beta\xi = 0.11$. It can be seen that the

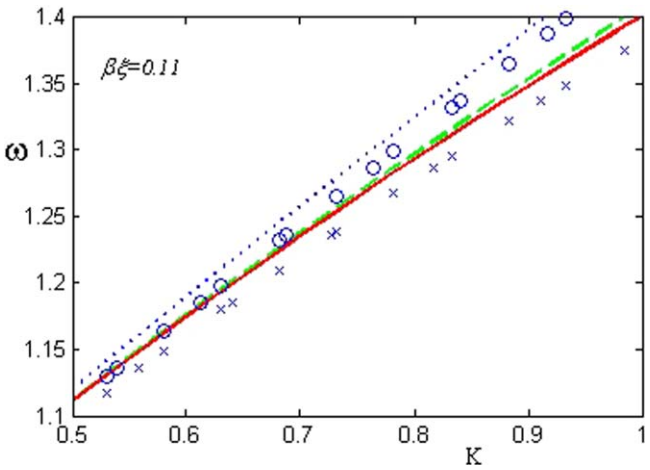

Figure 3. The normalized frequency of the surface Plasmon waves W with respect to the normalized wave number K, for different values of the Plasmonic coupling parameter H, as solid line refers to $H = 0.1$, dashed line refers to $H = 0.2$, and dotted line refer to $H = 0.5$. In this case $\beta\xi = 0.11$.

quantum effects beside the presence of boundary graphene layer cause to increase the wave frequency. Therefore, inclusion of the boundary graphene layer and quantum effects makes the Plasmon waves faster than that reported in the Ritchie limit [14].

It must be added that the results are significantly sensitive to the work frequency, as the graphene conductivity at high frequencies may be dominated by interband conductivity formulation. In this limit the effect of boundary graphene layer may be changed due to the interband conductivity.

4. Conclusions

In summary, we have employed a simple quantum hydrodynamic approach to investigate the dispersion properties of surface Plasmon waves in semi-infinite plasma in the presence of a boundary graphene layer. In this context, all the previous results are also recovered. At first approximation the garaphene layer leads to discreteness in electromagnetic fields at interface of plasma-vacuum. For typical numerical parameters corresponding to gold metal [16], the presence of graphene layer enhances the wave frequency as well as the phase velocity. This up-shift is similar to that causes by the quantum effects. Thus, inclusion of boundary graphene layer and quantum effects significantly affect the wave frequency relative to the Ritchie limit. Consideration of different physical parameters that yield other interesting plasma situations (such as degenerate plasma, relativistic plasma, etc) can be a problem of interest, but is beyond of the scope of the present study. Also, the coupling between the Plasmons in graphene and plasma regions may be left for future investigation. The results of present study must be contributed to the surface plasma and modern nano-electronic investigations.

References

[1] Alexandrov A F, Bogdankevich L S and Rukhadze A A 1984 *Principles of Plasma Electrodynamics* ed G Ecker *et al* (Berlin: Springer) p 302
[2] Stenflo L 1996 *Phys. Scr.* **T63** 59
[3] Aliev M Y, Schluter H and Shivarova A 2000 *Guided-Wave-Produced Plasmas* ed G Ecker *et al* (Berlin: Springer) p 29
[4] Stenflo L and Yu M Y 2003 *Phys. Plasmas* **10** 912
[5] Pathak N K, Pathak H, Pandey G K, Ji A and Sharma R P 2016 *Appl. Phys.* A **122** 1048
[6] Shoaib B, Haneef M, Khan H and Bakhtawar 2019 *Commun. Theor. Phys.* **71** 435
[7] Lezec H J, Degiron A, Devaux E, Linke R A, Martin-Moreno L, Garcia-Vidal F J and Ebbesen T W 2002 *Science* **297** 820
[8] Shalaev V M and Kawata S 2007 *Nanophotonics with Surface Plasmons* (Boston: Elsevier) p 141
[9] Ma Y T, Mao S H and Xue J K 2011 *Phys. Plasmas* **18** 102108
[10] Misra A P, Ghosh N K and Shukla P K 2010 *J. Plasma Phys.* **76** 87
[11] Moaied M, Tyshetskiy Y and Vladimirov S V 2013 *Phys. Plasmas* **20** 022116
[12] Ritchie R H 1957 *Phys. Rev.* **106** 874
[13] Trivelpiece A W and Gould R W 1959 *J. Appl. Phys.* **30** 1784
[14] Ritchie R H 1963 *Prog. Theor. Phys.* **29** 607
[15] Kaw P K and McBride J B 1970 *Phys. Fluids* **13** 1784
[16] Lazar M, Shukla P K and Smolyakov A 2007 *Phys. Plasmas* **14** 124501
[17] Shahmansouri M 2015 *Phys. Plasmas* **22** 092106
[18] Manfredi G 2005 *Fields Inst. Commun.* **46** 263
[19] Brey L, Dempsey J, Johnson N F and Halperin B I 1990 *Phys. Rev.* B **42** 1240
[20] Mohamed B F 2010 *Phys. Scr.* **82** 065502
[21] Moradi A 2015 *Phys. Scr.* **90** 085601
[22] Moradi A 2016 *Phys. Plasmas* **23** 084501
[23] Misra A P 2011 *Phys. Rev.* E **83** 057401
[24] Niknam A R, Boroujeni S T and Khorashadizadeh S M 2013 *Phys. Plasmas* **20** 122106
[25] Khorashadizadeh S M, Boroujeni S T, Rastbood E and Niknam A R 2012 *Phys. Plasmas* **19** 032109
[26] Zhu J, Zhao H and Qiu M 2013 *Phys. Lett.* A **377** 1736
[27] Tyshetskiy Y O, Vladimirov S V and Kompaneets R 2013 *J. Plasma Phys.* **79** 387
[28] Zhu J 2015 *J. Plasma Phys.* **81** 905810110
[29] Misra A P 2007 *Phys. Plasmas* **14** 064501
[30] Shahmansouri M, Farokhi B and Aboltaman R 2017 *Phys. Plasmas* **24** 054505
[31] Moradi A 2015 *Phys. Plasmas* **22** 014501
[32] Shahmansouri M and Mahmodi Moghadam M 2017 *Phys. Plasmas* **24** 102107
[33] Shahmansouri M and Misra A P 2016 *Phys. Plasmas* **23** 072105
[34] Bonaccorso F, Sun Z, Hasan T and Ferrari A C 2010 *Nat. Photon.* **4** 611
[35] Geim A K 2011 *Rev. Mod. Phys.* **83** 851
[36] Novoselov K S, Geim A K, Morozov S V, Iang D J, Hang Y Z, Dubonos S V, Grigorieva I V and Firsov A A 2004 *Science* **306** 666
[37] Ye S, Wei B, Sun C, Dong C and Jian S 2017 *Appl. Phys.* A **123** 637
[38] Fei Z *et al* 2013 *Nat. Nanotechnol.* **8** 821
[39] Li Z Q, Henrikse E A, Jiang Z, Hao Z, Martin M C, Kim P, Stormer H L and Basov D N 2008 *Nat. Phys.* **4** 532
[40] Neto A H C, Guinea F, Peres N M R, Novoselov K S and Geim A K 2009 *Rev. Mod. Phys.* **81** 109
[41] Liu S, Zhang C, Hu M, Chen X, Zhang P, Gong S, Zhao T and Zhong R 2014 *Appl. Phys. Lett.* **104** 201104

[42] Bonaccorso F, Lombardo A, Hasan T, Sun Z, Colombo L and Ferrari A C 2012 *Mater. Today* **15** 564
[43] Shahmansouri M, Aboltaman R and Misra A P 2018 *Phys. Lett.* A **382** 2133
[44] Chorsi M T and Chorsi H T 2017 *Appl. Phys.* A **123** 757
[45] Stauber T, Peres N M R and Geim A K 2008 *Phys. Rev.* B **78** 085432
[46] Gusynin V P, Sharapov S G and Carbotte J P 2007 *Phys. Rev.* B **75** 165407
[47] Bao Q and Loh K P 2012 *ACS Nano* **6** 3677
[48] Vakil A and Engheta N 2011 *Science* **332** 1291
[49] Horng J *et al* 2011 *Phys. Rev.* B **83** 165113
[50] Wang B, Zhang X, Yuan X and Teng J 2012 *Appl. Phys. Lett.* **100** 131111
[51] Hanson G W 2008 *J. Appl. Phys.* **103** 064302
[52] Liu S, Zhang C, Hu M, Chen X, Zhang P, Gong S, Zhao T and Zhong R 2014 *Appl. Phys. Lett.* **104** 201104
[53] Geim A K and Novoselov K S 2007 *Nat. Mater.* **6** 183
[54] Xu Z and Buehler M J 2010 *J. Phys.: Condens. Mater.* **22** 485301
[55] Najafianpour N and Dorranian D 2018 *Appl. Phys.* A **124** 805
[56] Giovannetti G, Khomyakov P A, Brocks G, Karpan V M, van den Brink J and Kelly P J 2008 (arXiv:0802.2267v3 [cond-mat.mtrl-sci])
[57] Sutter P W, Flege J I and Sutter E A 2008 *Nat. Mater.* **7** 406
[58] Mitzayé Del Castillo R and Sansores L E 2015 *Eur. Phys. J.* B **88** 248
[59] Manfredi G and Haas F 2001 *Phys. Rev.* B **64** 075316